Weak Incoherent Optical Signal Amplification Based on Modulation Instability for Imaging Through Fog

Zhaolu Wang, Yongbin Zhang, Nan Huang, Yuan Liao, Changchang Zhang, Xiaohui Gao, and Hongjun Liu

***Abstract*—Weak optical signal processing based on nonlinear effects offers new approaches for imaging through scattering media. A novel incoherent optical signal amplification method based on spatial modulation instability is proposed for imaging through fog. We experimentally demonstrated the amplification and recovery of degraded weak incoherent optical image signals after passing through dense fog in a photorefractive crystal. Our experimental results indicate that the intensity profiles of the output images can be redistributed from disordered to ordered when the nonlinear strength exceeds the threshold of incoherent modulation instability, which shows that the partially disordered incoherent probe light intensities are orderly transferred to enhance the signal intensity profiles and the residuals become a uniform background. The restored nonlinear output images with high visibility were observed for a proper optical thickness of fog, and weak optical imaging from undetectable to detectable with relatively poor visibility for a larger optical thickness was also realized in the experiment. This incoherent optical signal amplification method based on modulation instability has a potential application for image recovery in atmospheric scattering imagings.**

***Index Terms*—Incoherent optical amplification, spatial modulation instability, fog, disordered, scattering imaging.**

I. Introduction

TO DATE, optical imaging through scattering media remains a fundamental problem, especially for imaging in degraded visual environments, such as atmospheric imaging, or underwater imaging [1]–[7]. When an imaging beam passes through the scattering media, the output beam contains the signal light (ballistic light) and scattered light. The signal photons are reduced exponentially and the scattered photons increase as the optical thickness of the scattering media increases due to the absorption and scattering effects, hence the signal-to-noise ratio (SNR) becomes increasingly lower until the signal power is too weak to be detected by the camera. In this case, linear filtering approaches will be ineffective. Nonlinear image signal processing technologies offer new ways for weak optical imaging with a low SNR. For example, the phase-sensitive optical parametric amplification (PS-OPA) based on second order nonlinearity enables noise-free amplification [8], which can be used to amplify the weak optical image signal and enhance the SNR. The PS-OPA depends on the relative phase between the pump, signal and idler, which means that this nonlinear method is only applied to coherent optical signal amplification. Therefore, it is a difficult challenge for incoherent optical signal amplification due to the random instantaneous variation of the amplitude and phase.

Significantly, weak optical nonlinear signal processing based on the photorefractive effect has potential applications in incoherent optical imaging through scattering media. Diffraction and self-focusing are the two main effects when the incoherent beam passes through the photorefractive crystal. For a broad beam, small amplitude and phase perturbations grow exponentially, and the beam tends to disintegrate during propagation with the interplay of diffraction and self-focusing, which means that the spatial modulation instability (MI) occurs [9]–[12]. Then the beam breaks up into dot filaments due to transverse instability [13], which even tend to form trains of solitons when the diffraction is balanced by nonlinear self-focusing [9], [12]. Therefore, the spatial MI can be considered as a precursor to soliton formation. In the last two decades, the incoherent (including partially incoherent light and incoherent white light) soliton and MI have been demonstrated theoretically and experimentally [9]–[12], [14]–[17], and have been explored in the area of imaging processing [18]–[20]. However, few works have investigated the weak optical nonlinear signal processing applied to atmospheric scattering imaging.

Here, we develop a novel weak incoherent optical signal amplification method aiming at providing vision assistance to identify faint target signals in degraded visual environments that are too weak to be detected by the camera. We experimentally demonstrated that the degraded weak image signals induced by absorption and scattering of dense fog can be amplified and recovered with the assistance of incoherent probe light based on

Manuscript received January 8, 2022; revised February 23, 2022; accepted March 8, 2022. Date of publication March 15, 2022; date of current version April 7, 2022. This work was supported in part by the Qingdao National Laboratory for Marine Science and Technology under Grant QNLM2016ORP0111, in part by National Natural Science Foundation under Grants 61975232 and 61775234, and in part by Youth Innovation Promotion Association CAS under Grant 2020398. *(Corresponding authors: Zhaolu Wang; Hongjun Liu.)*

Zhaolu Wang, Nan Huang, Yuan Liao, and Changchang Zhang are with the State Key Laboratory of Transient Optics and Photonics, Xi'an Institute of Optics and Precision Mechanics, Chinese Academy of Science, Xi'an 710119, China (e-mail: wangzhaolu@opt.ac.cn; huangnan@opt.ac.cn; liaoyuan18@mails.ucas.ac.cn; zhangchangchang2017@opt.cn).

Xiaohui Gao is with CAS Key Laboratory of Spectral Imaging Technology, Xian Institute of Optics and Precision Mechanics, CAS, Xian 710119, China (e-mail: gaoxhui@163.com).

Yongbin Zhang was with State Key Laboratory of Transient Optics and Photonics, Xi'an Institute of Optics and Precision Mechanics, Chinese Academy of Science, Xi'an 710119, China. He is now with China Airborne Missile Academy, Luoyang 471009, China (e-mail: zhangyongbin2015@163.com).

Hongjun Liu is with State Key Laboratory of Transient Optics and Photonics, Xian Institute of Optics and Precision Mechanics, Chinese Academy of Science (CAS), Xian 710119, China, and also with the Collaborative Innovation Center of Extreme Optics, Shanxi University, Taiyuan 030006, China (e-mail: liuhongjun@opt.ac.cn).

Digital Object Identifier 10.1109/JPHOT.2022.3158653

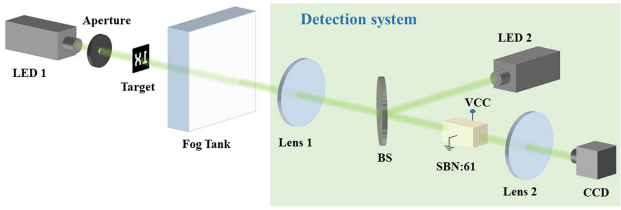

Fig. 1. Experimental setup of the nonlinear detection system for weak optical image signals through dense fog.

incoherent spatial MI in a self-focusing photorefractive crystal. The new phenomenon of the intensity profiles from disordered to ordered for the nonlinear output images is observed in the experiment for the first time, to the best of our knowledge. Our results show that this incoherent optical signal amplification method has potential application for image recovery in atmospheric scattering imaging.

II. Experiment

The experimental setup of the nonlinear detection system for weak optical imaging through dense fog is shown in Fig. 1. In our experiment, a collimating incoherent imaging beam is generated by a light-emitting diode (LED1) with a center wavelength of 530 nm and bandwidth of 35 nm. An aperture is used to control the beam size and adjust the coherent length of the incoherent light. After illuminating a 1951 USAF test target, the imaging beam carried the target information passes through a fog tank constructed with high-transmission organic glass. The tank is filled with fog, which is generated by an ultrasonic atomizer, and the diameter of the fog drop is approximately 1 μm. The concentration of fog can be changed by tuning the electrical power of the ultrasonic atomizer. The degraded imaging beam through the fog is incident onto an SBN:61 ($Sr_{0.61}Ba_{0.39}Nb_2O_6$, doped with CeO_2) crystal with applied voltage (V) across the c-axis after passing through an imaging lens (Lens 1) and a beam splitter (BS). The dimensions of the crystal are 5.5 mm $\times$ 10 mm $\times$ 5 mm with a distance along the c-axis of $d = 5$ mm and the light propagation distance of $L = 10$ mm. The degraded beam inside the crystal contains a weak signal and scattering noise, and the noise is also very weak due to the large scattering angle induced by the fog drop. By tuning the applied voltage, the weak signal of the degraded incoherent beam induces a nonlinear index change in the crystal due to the photorefractive effect, and the incoherent MI occurs when the nonlinear index change (Δn) exceeds a threshold. The nonlinear index change is given by $\Delta n = -0.5{n_e}^3\, r_{33}E\langle I\rangle/(1+\langle I\rangle)$ [21], where $n_e = 2.2817$ is the extraordinary refractive index of the photorefractive crystal, $E = -V/d$ is the electric field intensity, and $r_{33} = 250$ pm/V is the electro-optic coefficient. $\langle I\rangle$ is the time-averaged optical intensity in the non-instantaneous nonlinear media. With increasing nonlinearity, a graded refractive index waveguide will be created by the weak nonlinearity, and the scattering noise will transfer to the waveguide. Since the output signal is so weak and even undetectable by the charge-coupled device (CCD) camera, a broadband incoherent light as a probe light (or background light) generated by LED2 at a wavelength centered at 520 nm is provided in the nonlinear detection system to amplify the weak signal. MI in photorefractive crystals can be controlled through the intensity ratio of background to signal fields [22]. The probe light is collinear with the weak signal inside the crystal by tuning the BS, and partially probe light intensities are transferred and limited to the graded refractive index waveguide to amplify the weak signal. The output from the crystal is then imaged onto a CCD camera.

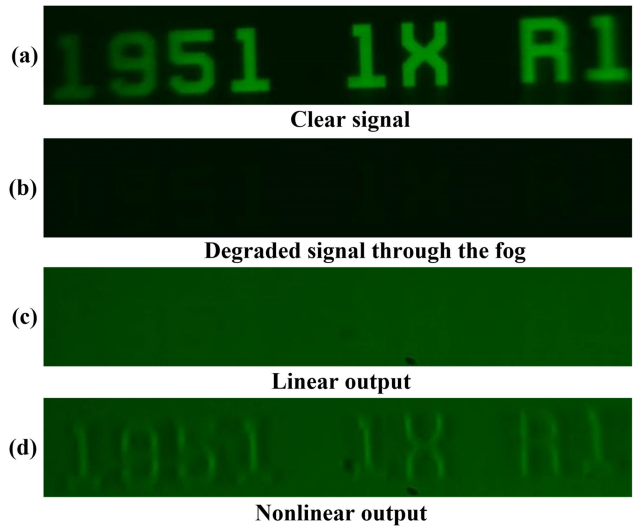

Fig. 2. The images observed in the experiment. (a) The clear image signal; (b) The degraded signal through the fog, which is nearly undetectable; (c) The linear output image with probe light for E = 0 V/cm; (d) The nonlinear output image with probe light for E = 6400 V/cm.

In the experiment, the optical thickness of fog can be changed by tuning the concentration of fog, which is represented by the attenuation lengths (ALs). The attenuation length is given by AL $= 1/C$, where $C = \alpha+\gamma$ is the total attenuation coefficient, α is the absorption coefficient and γ is the scattering coefficient. The incoherent probe light power is approximately 2 μW, and the intensity ratio of probe light and weak signal inside the crystal is measured as $I_p/I_s \approx 10{:}1$. Fig. 2(a) shows the 1951 USAF test target signal without fog, which is very clear. When the optical thickness (OT) of the fog is 3.91 AL, the degraded image signal induced by absorption and scattering is nearly undetectable by the CCD, which is depicted in Fig. 2(b). In this case, the average optical intensity of the attenuated signal is also larger than the average optical intensity of the scattering noise with $I_s/I_n > 1$. Then, we used the incoherent probe light to amplify and recover the degraded signal via weak nonlinearity. When the electric field intensity $E = 0$ V/cm, the linear output shows that the degraded weak signal is completely obscured by the incoherent probe light due to the nonlinear index change $\Delta n = 0$, which is totally unidentifiable as shown in Fig. 2(c). When the electric field intensity $E = 6400$ V/cm, a graded refractive index waveguide is created via the seeded MI effect, and the partially incoherent probe light intensities are transferred to the waveguide along the crystal, hence the nonlinear output shows that the weak signal is amplified and the image is recovered with better visibility as illustrated in Fig. 2(d).

III. Results and Discussion

To analyze the process of weak incoherent optical signal amplification and image recovery via weak nonlinearity, we

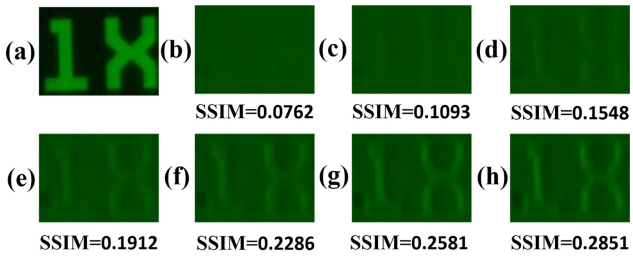

Fig. 3. Experimental observation of output images at different electric field intensities. (a) The target image signal; (b) the linear output image E = 0 V/cm; (c)-(h) the nonlinear output image for E = 2400 V/cm, E = 3200 V/cm, E = 4000 V/cm, E = 4800 V/cm, E = 5600 V/cm, E = 6400 V/cm, respectively.

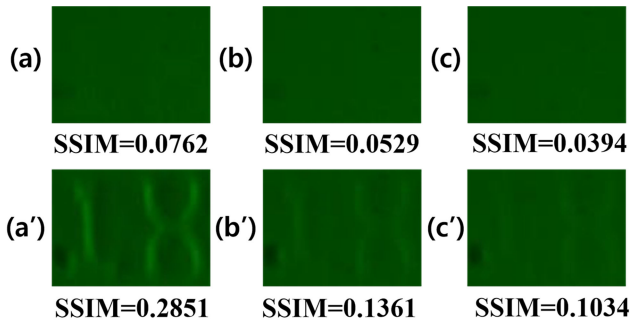

Fig. 4. Experimental observation of output images with different optical thicknesses of fog for a fixed electric field intensity E = 6400 V/cm. (a) The linear output image and (a') the nonlinear output image for OT = 3.91 AL; (b) The linear output image and (b') the nonlinear output image for OT = 4.28 AL; (c) The linear output image and (c') the nonlinear output image for OT = 4.42 AL.

observed the output images at different electric field intensities for a fixed optical thickness of 3.91 AL as shown in Fig. 3. We used the structural similarity (SSIM) index to evaluate the image quality of the output images [23]. The unrecognized linear output image is shown in Fig. 3(b), for which there are no incoherent probe light energies redistributed to amplify the weak signal due to the instability gain $g = 0$, and the degraded weak signal is completely obscured by the incoherent background light. For nonlinear output, the image quality improves as the electric field intensity increases, which means that the graded refractive index waveguide is created and the refractive index contrast becomes larger with the increase of nonlinear index change after the nonlinear strength is above the MI threshold. When the electric field intensity $E = 2400$ V/cm, the nonlinear output image with poor visibility with SSIM = 0.1093 is shown in Fig. 3(c), for which fewer probe light energies are transferred to amplify the weak signal owing to the instability threshold is just attained. When the electric field intensity $E = 6400$ V/cm, a large proportion of probe light energies are transferred and limited in the graded refractive index waveguide to amplify and recover the weak optical image signal, and the output image has a better visibility with SSIM = 0.2851 as shown in Fig. 3(h).

Then, we changed the concentration of fog, which is expressed by the optical thickness, to investigate the degraded weak optical signal amplification and image recovery based on the weak nonlinearity. The linear and nonlinear output images with different optical thicknesses of fog are shown in Fig. 4. The degraded weak image signals are obscured by the strong

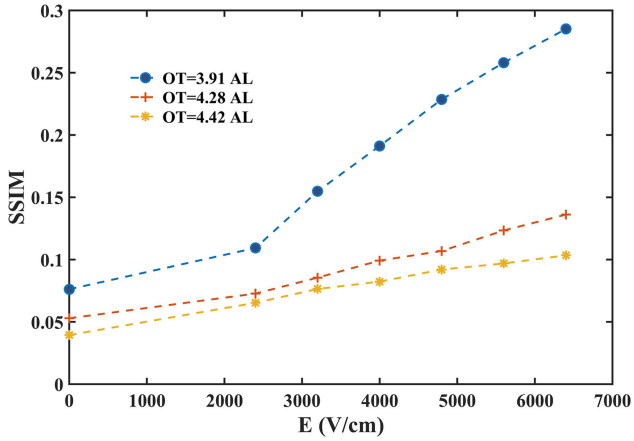

Fig. 5. SSIM index versus electric field intensity for different optical thickness.

incoherent probe light for all the linear output images, which are unrecognizable as depicted by Fig. 4(a)–(c). For a fixed electric field intensity $E = 6400$ V/cm, nonlinear output images are visible due to the weak signal amplification by coupling the strong incoherent probe light, but the image quality decreases with increasing concentration of fog as shown in Fig. 4(a')–(c'). When the optical thickness of fog is 4.42 AL, the value of the SSIM index is only 0.1034 for the recovered image, which is similar to the output image at $E = 2400$ V/cm for OT = 3.91 AL as shown in Fig. 3(c). This result indicates that the MI threshold increases as the concentration of the fog increases, because the optical intensity of the image signal becomes weaker, and the coherent length of the scattering noise decreases due to the strong multiple scattering for thicker fog. For a larger optical thickness of the fog, the SSIM of the nonlinear output images is less than 0.1 for $E = 6400$ V/cm, which means that the output images are unrecognized when the optical thickness of the fog is greater than 4.42 AL in this work. Therefore, the method we proposed can achieve imaging through fog with a maximum OT of 4.42 AL in this experiment.

The comparison of the nonlinear output image quality for different optical thickness are shown in Fig. 5. The SSIM index increases with increasing electric field intensity, and the improvement is very significant for OT = 3.91 AL. For a given electric field intensity, the SSIM index decreases with increasing optical thickness of the fog. Because the spatial coherence of the input beam decreasing with increasing the concentration of the fog, which will decrease the MI growth rate and even decrease it to below the threshold. Therefore, larger optical thickness will limit the improvement of the nonlinear output images.

To better understand the process of weak signal amplification and image recovery based on incoherent MI, Fig. 6 shows the three-dimensional intensity profiles of linear and nonlinear output images with different optical thicknesses of fog, which are the same as the images of Fig. 4. It is shown that the intensity profiles of linear out images are random and disordered, because the weak signals and random scattering noises induced by fog are overwhelmed by the strong incoherent probe light for which the amplitude and phase are disordered. For the nonlinear output images with electric field intensity $E = 6400$ V/cm, the

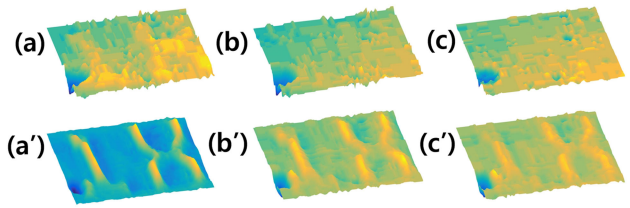

Fig. 6. The three-dimensional intensity profiles of output images with different optical thicknesses of fog for a fixed electric field intensity E = 6400 V/cm. (a) The linear and (a') nonlinear output for OT = 3.91 AL; (b) The linear and (b') nonlinear output for OT = 4.28 AL; (c) The linear and (c') nonlinear output for OT = 4.42 AL.

TABLE I
COMPARISON OF THE IMAGE QUALITY FOR INPUT AND OUTPUT IMAGES

E=6400 V/cm		Input	Linear output	Nonlinear output	Maximum increment
OT=3.91AL	SSIM	0.0322	0.0762	0.2851	0.2529
	PSNR [dB]	11.76	14.74	15.65	3.89
OT=4.28AL	SSIM	0.0182	0.0529	0.1361	0.1179
	PSNR [dB]	11.62	14.65	15.03	3.41
OT=4.42AL	SSIM	0.016	0.0394	0.1034	0.0874
	PSNR [dB]	11.6	14.59	14.85	3.25

intensity profiles are shown in Fig. 6(a')–(c'), which shows that the intensity profiles of the incoherent probe light become a uniform background while the intensity profiles of the signal are amplified with an apparent boundary through the redistribution of the partially disordered probe light intensities induced by the graded refractive index waveguide in the nonlinear crystal, especially for the intensity profiles when the optical thickness of fog is 3.91 AL as illustrated in Fig. 6(a'). With increasing optical thickness, Fig. 6(b') and (c') show that the contrast between the signal intensity profiles and the background profiles is reduced due to the decrease of the nonlinear strength, which exhibits poor visibility of the restored images as shown in Fig. 4(b') and (c'). This indicates that weak nonlinear signal processing can enable the intensity profiles from disordered to ordered via the nonlinear MI effect, and the contrast of the intensity profiles is limited by a larger optical thickness of scattering media. Therefore, it is demonstrated that the degraded weak optical image signal can be amplified and recovered with high visibility by the incoherent probe light via weak nonlinearity when the optical thickness of the scattering media is appropriate. Specifically, this nonlinear method can also realize the weak signal imaging through scattering media from undetectable to detectable for a larger optical thickness despite poor visibility, such as the image shown in Fig. 6(c') for OT = 4.42 AL in this experiment.

To better evaluate the effectiveness of the method, we give the value of SSIM and peak signal-to-noise ratio (PSNR) [24] for input images, linear output images and nonlinear output images when the optical thickness of the fog is difference, as listed in Table I. Compared with the value of input images, the maximum increment of SSIM for output images is 0.2529, and the maximum increment of PSNR is 3.89 dB for OT = 3.91 AL. The maximum increment decreases with the optical thickness of the fog increases. When the optical thickness is 4.42 AL, the maximum increment of SSIM is only 0.0874, while the maximum increment of PSNR is 3.25 dB. This reflects that the evaluation result of SSIM is more consistent with the human visual system.

V. CONCLUSION

We have experimentally demonstrated the weak incoherent signal amplification and image recovery via weak nonlinearity for imaging through fog. The degraded weak signal containing scattering noise transmitted in the photorefractive crystal can occur incoherent MI when the nonlinear strength is above the instability threshold, which will create a graded refractive index waveguide inside the crystal. Then, incoherent probe light is used to amplify and recover the weak image signal, as partially probe light intensities are transferred and limited to the graded refractive index waveguide. The nonlinear output image quality improves as the electric field intensity increases after the nonlinear strength is above the MI threshold for a fixed fog concentration, and the restored image quality reduces with increasing fog concentration because the MI threshold increases. Moreover, we also demonstrated that the weak nonlinear signal processing can enable the intensity profiles of the output images to change from disordered to ordered, for which the partially disordered incoherent probe light intensities are orderly transferred to enhance the signal intensity profiles and the residuals become uniform background intensity profiles. For a proper optical thickness, our incoherent optical amplification method can recover the degraded weak image signal with high visibility, and it can also realize the weak optical imaging from undetectable to detectable even for a larger optical thickness of scattering media, which will have potential applications for atmospheric imaging, or underwater imaging. Next, we will investigate the weak signal amplification of the natural light for atmospheric imaging of passive lighting, which will have important applications in the field of optical remote sensing.

REFERENCES

[1] J. Bertolotti, E. G. van Putten, C. Blum, A. Lagendijk, W. Vos, and A. P. Mosk, "Non-invasive imaging through opaque scattering layers," *Nature*, vol. 491, no. 7423, pp. 232–234, Nov. 2012, doi: 10.1038/nature11578.
[2] S. Popoff, G. Lerosey, M. Fink, A. C. Boccara, and S. Gigan, "Image transmission through an opaque material," *Nat. Commun.*, vol. 1, pp. 1–5, Sep. 2010, doi: 10.1038/ncomms1078.
[3] R. N. Mahalati and J. M. Kahn, "Effect of fog on free-space optical links employing imaging receivers," *Opt. Exp.*, vol. 20, no. 2, pp. 1649–1661, Jan. 2012, doi: 10.1364/OE.20.001649.
[4] S. Jaruwatanadilok, A. Ishimaru, and Y. Kuga, "Optical imaging through clouds and fog," *IEEE Trans. Geosci. Remote Sens.*, vol. 41, no. 8, pp. 1834–1843, Aug. 2003, doi: 10.1109/TGRS.2003.813845.
[5] A. Kanaev *et al.*, "Imaging through extreme scattering in extended dynamic media," *Opt. Lett.*, vol. 43, no. 13, pp. 3088–3091, Jul. 2018, doi: 10.1364/OL.43. 003088.
[6] J. Y. Chiang and Y. C. Chen, "Underwater image enhancement by wavelength compensation and dehazing," *IEEE Trans. Image Process.*, vol. 21, no. 4, pp. 1756–1769, Apr. 2012, doi: 10.1109/TIP.2011.2179666.
[7] F. Liu *et al.*, "Deeply seeing through highly turbid water by active polarization imaging," *Opt. Lett.*, vol. 43, no. 20, pp. 4903–4906, Oct. 2018, doi: 10.1364/OL. 43.004903.

[8] S. K. Choi, M. Vasilyev, and P. Kumar, "Noiseless optical amplification of images," *Phys. Rev. Lett.*, vol. 83, no. 10, pp. 1938–1941, Sep. 1999, doi: 10.1103/PhyRevLett.83.1938.

[9] D. Kip, M. Soljacic, M. Segev, E. Eugenieva, and D. N. Christodoulides, "Modulation instability and pattern formation in spatially incoherent light beams," *Science*, vol. 290, no. 5491, pp. 495–498, Oct. 2000, doi: 10.1126/science.290.5491.495.

[10] M. Soljacic, M. Segev, T. Coskun, D. N. Christodoulides, and A. Vishwanath, "Modulation instability of incoherent beams in noninstantaneous nonlinear media," *Phys. Rev. Lett.*, vol. 84, no. 3, pp. 467–470, Jan. 2000, doi: 10.1103/PhyRevLett.84.467.

[11] H. Buljan, A. Šiber, M. Soljačić, and M. Segev, "Propagation of incoherent 'white' light and modulation instability in noninstantaneous nonlinear media," *Phys. Rev. E*, vol. 66, no. 3, Sep. 2002, Art. no. 035601, doi: 10.1103/PhyRevE.66.035601.

[12] T. Schwartz, T. Carmon, H. Buljan, and M. Segev, "Spontaneous pattern formation with incoherent white light," *Phys. Rev. Lett.*, vol. 93, no. 22, Nov. 2004, Art. no. 223901, doi: 10.1103/PhyRevLett.93.223901.

[13] C. C. Jeng, Y. Y. Lin, R. C. Hong, and R. K. Lee, "Optical pattern transitions from modulation to transverse instabilities in photorefractive crystals," *Phys. Rev. Lett.*, vol. 102, no. 15, Apr. 2009, Art. no. 153905, doi: 10.1103/PhyRevLett.102.153905.

[14] D. V. Dylov and J. W. Fleischer, "Modulation instability of a coherent-incoherent mixture," *Opt. Lett.*, vol. 35, no. 13, pp. 2149–2151, Jul. 2010, doi: 10.1364/OL.35.002149.

[15] D. Anderson, L. Helczynski-Wolf, M. Lisak, and V. E. Semenov, "Features of modulational instability of partially coherent light: Importance of the incoherence spectrum," *Phys. Rev. E*, vol. 69, no. 2, Feb. 2004, Art. no. 025601, doi: 10.1103/PhyRevE.69.025601.

[16] C. Sun, L. Waller, D. V. Dylov, and J. W. Fleischer, "Spectral dynamics of spatially incoherent modulation instability," *Phys. Rev. Lett.*, vol. 108, no. 26, Jun. 2012, Art. no. 263902, doi: 10.1103/PhyRevLett.108.263902.

[17] D. R. Solli, G. Herink, B. Jalali, and C. Ropers, "Fluctuations and correlations in modulation instability," *Nat. Photon.*, vol. 6, no. 7, pp. 463–468, Jul. 2012, doi: 10.1038/NPHOTON.2012.126.

[18] D. V. Dylov and J. W. Fleischer, "Nonlinear self-filtering of noisy images via dynamical stochastic resonance," *Nat. Photon.*, vol. 4, no. 5, pp. 323–328, May 2010, doi: 10.1038/NPHOTON.2010.31.

[19] D. V. Dylov, L. Waller, and J. W. Fleischer, "Instability-driven recovery of diffused images," *Opt. Lett.*, vol. 36, no. 18, pp. 3711–3713, Sep. 2011, doi: 10.1364/OL.36.003711.

[20] Z. Wang, H. Liu, N. Huang, Y. Zhang, and J. Chi, "Nonlinear reconstruction of weak optical diffused images under turbid water," *Opt. Lett.*, vol. 44, no. 14, pp. 3502–3505, Jul. 2019, doi: 10.1364/OL.44.003502.

[21] C. Sun, D. V. Dylov, and J. W. Fleischer, "Nonlinear focusing and defocusing of partially coherent spatial beams," *Opt. Lett.*, vol. 34, no. 19, pp. 3003–3005, Oct. 2009, doi: 10.1364/OL.34.003003.

[22] C. C. Jeng, Y. SU, R. C. Hong, and R. K. Lee, "Control modulation instability in photorefractive crystals by the intensity ratio of background to signal fields," *Opt. Exp.*, vol. 23, no. 8, pp. 10266–10271, Apr. 2015, doi: 10.1364/OE.23.010266.

[23] Z. Wang, A. C. Bovik, H. R. Sheikh, and E. P. Simoncelli, "Image quality assessment: From error visibility to structural similarity," *IEEE Tran. Imag. Process.*, vol. 13, no. 4, pp. 600–612, Apr. 2004, doi: 10.1109/TIP.2003.819861.

[24] A. Tanchenko, "Visual-PSNR measure of image quality," *J. Vis. Commun. Image R.*, vol. 25, no. 5, pp. 874–878, Jul. 2014, doi: 10.1016/j.jvcir.2014.01.008.